Plant Soil (2026) 523:791–810
https://doi.org/10.1007/s11104-024-07069-9

RESEARCH ARTICLE

Metabolomics and dual proteomics identify contrasting patterns of major pathways affected in asparagus shoot upon Fusarium infection

Katja Witzel · Roxana Djalali Farahani-Kofoet · Stefanie Döll · Viktoria Lindemann · Benedikt Cramer · Hans-Ulrich Humpf · Rita Zrenner

Received: 5 June 2024 / Accepted: 31 October 2024 / Published online: 19 November 2024
© The Author(s) 2024

Abstract

Aims Infections with soil-borne pathogens have considerable detrimental effects on asparagus (*Asparagus officinalis*) growth and production, notably caused by the Fusarium species *F. oxysporum* f.sp. *asparagi*, *F. proliferatum,* and *F. redolens*. To get insight into the systemic effects of fungal infection on plant physiology to identify candidate resistance traits, we investigated this interaction using a multi omics approach.

Methods Asparagus plants were inoculated with one of the three Fusarium species. After 8 weeks, basal stem parts were harvested and subjected to metabolome and proteome analysis as well as detection of fungal DNA.

Results Upon infection, the pathogen spreads systemically from the root to the shoot and, consequently, fungal DNA and mycotoxins were detected in the basal part of the plant stem. Metabolite data revealed that the main pathway affected by Fusarium infections was "Fatty acids", specifically the superclasses "Glycerophospholipids", "Glycerolipids" and "Sphingolipids" being lower abundant upon infection. Another main pathway identified in the analysis was "Shikimates and Phenylpropanoids" with compounds assigned to these classes being mainly enriched upon infection. Proteome data revealed an induction of pathogen-defense proteins upon infection in asparagus, while proteins involved in vesicle trafficking and lipid metabolism were lower abundant.

Conclusions This indicates that not only lipid-based signaling processes are distorted by Fusarium, but also fundamental processes such as vesicle formation, membrane integrity and cell wall organization. *In planta* proteome analysis of *F. oxysporum* led to the identification of 1,488 fungal proteins, including proteins involved in metabolic and cellular processes as well as putative virulence factors.

Keywords *Asparagus officinalis* · Phytopathogenic fungi · *Fusarium* crown and root rot · Metabolomics · Mycotoxin · Proteomics

Responsible Editor: Martha Isabel Gomez Alvarez.

Supplementary Information The online version contains supplementary material available at https://doi.org/10.1007/s11104-024-07069-9.

K. Witzel (✉) · R. Djalali Farahani-Kofoet · R. Zrenner
Leibniz Institute of Vegetable and Ornamental Crops, Theodor-Echtermeyer-Weg 1, 14979 Großbeeren, Germany
e-mail: witzel@igzev.de

S. Döll
German Centre for Integrative Biodiversity Research Halle-Jena-Leipzig, Deutscher Platz 5E, 04103 Leipzig, Germany

V. Lindemann · B. Cramer · H.-U. Humpf
Institute of Food Chemistry, Universität Münster, Corrensstrasse 45, 48149 Münster, Germany

Abbreviations

FB	Fumonisin
BEA	Beauvericin
ENN	Enniatin
PAL	Phenylalanine ammonium lyase
PR	Pathogenesis-related
LC-MS	Liquid-chromatography mass spectrometry

Introduction

Asparagus (*Asparagus officinalis*) is a perennial vegetable produced worldwide, with a high nutritional value and low-calorie intake. Green and white spears are rich in antioxidants, such as polyphenols, flavonoids and ascorbic acid as well as amino acids (Lee et al. 2014; Creydt et al. 2018a; Jiménez-Sánchez et al. 2016; Ku et al. 2018). Roots are traditionally used as a medicinal product, mainly due to their accumulation of saponins and fructans (Iqbal et al. 2017; Zhang et al. 2019). In order to maintain high productivity, asparagus requires replanting after about 10–15 years and the high failure rate associated with replanting new crops in old asparagus fields is an important problem for producers. Asparagus cultivation is affected by soil-borne pathogenic Fusarium species, which cause yield losses during the typical 10-year cultivation period. These species include *F. oxysporum* f. sp. *asparagi*, *F. proliferatum*, and *F. redolens* f.sp. *asparagi*, all of which cause necrotic lesions on root and stem surfaces, rot on roots, rhizomes and stems, and a reduction in plant size and wilting of ferns (Baayen et al. 2000; Elmer 1990; Lamondia and Elmer 1989). *F. oxysporum* and *F. proliferatum* were found in the epidermis and parenchyma cells of green (Andrzejak & Janowska 2022) and white spears (Andrzejak and Janowska 2021), indicating their capability to colonize all tissues of spears and spread systemically within the plant. Fusarium-caused crown and root rot is difficult to control because the pathogen is soil-borne, the crop is perennial and highly resistant cultivars are not available (Jacobi et al. 2023). Hence, a better understanding of Fusarium-induced modifications in plant metabolism would lead to the identification of new biomarkers for the improvement of crop resistance.

Fusarium belongs to the genera of plant pathogenic fungi that cause the greatest economic damage due to spoilage of feed and food stocks with mycotoxins. For example, *F. graminearum* infection of cereals leads to the accumulation of the sesquiterpenes trichothecenes (e.g. deoxynivalenol) in grains, that have toxic effects on animals and plants (Munkvold 2017). *F. proliferatum* and *F. oxysporum* can form a variety of mycotoxins, including moniliformin, a semisquaric acid sodium salt, fumonisins (FBs), which are polyketides, and beauvericin (BEA) and enniatins (ENNs), both being structurally similar cyclohexadepsipeptides. So far, only BEA was detected in *F. redolens* (Urbaniak et al. 2020). Also, these mycotoxins are associated with toxicoses in humans and livestock (Munkvold 2017). Infection of asparagus with *F. proliferatum* leads to the accumulation of up to 4.5 mg/g FB1 in heavily infected spears grown under field conditions (Seefelder et al. 2002). In a greenhouse experiment, asparagus plants infected with *F. proliferatum* and *F. oxysporum* accumulated FB1 and moniliformin in roots and stems, with FB1 being more abundant in roots and moniliformin being higher concentrated in the stem four weeks after the infection (Waskiewicz et al. 2013). During plant infection, mycotoxins are important pathogenicity factors that interfere with the plant's metabolism. Due to structural similarity, FB1 disrupts sphingolipid biosynthesis by blocking ceramide synthase resulting in an accumulation of cytotoxic intermediates (Zeng et al. 2020). Sphingolipids are structural components of membranes and second messengers in signaling events and, hence, FB1 affects membrane integrity, hormone and calcium signaling, and leads to increased autophagy and reactive oxygen species (Zeng et al. 2020; Lanubile et al. 2022). Only little is known on the effect of BEA and ENNs on host physiology. Treatment of plants with BEA leads to depolarization of the plasma membrane, accompanied by potassium leakage, and depletion of extracellular ATP (Pavlovkin et al. 2012; Srobarova et al. 2009), due to its ability to form channels in membranes (Mallebrera et al. 2018). This is accompanied by induction of reactive oxygen species (ROS) and activation of ROS scavenging enzymes and metabolites (Loi et al. 2020). ENNs are also known to possess ionophoric activity (Sy-Cordero et al. 2012) and therefore, similar effects during plant pathogenesis can be expected.

Wild relatives of *A. officinalis* seem to be more resistant against Fusarium infection as compared to asparagus cultivars. *A. densiflorus* and *A. aethiopicus* showed high resistance in a seedling inoculation test,

which was accompanied by accumulation of hydrogen peroxide in roots cells, while this was not observed in susceptible *A. officinalis* cultivars (Jacobi et al. 2023). Increased resistance in *A. densiflorus* is due to the induction of hypersensitive response and necrosis in root cells, rapid and strong induction of peroxidase activity in roots and spears, and high increase in phenylalanine ammonium lyase (PAL) activity in roots (He et al. 2002). In susceptible *A. officinalis* cultivars, expression of peroxidase and PAL rather decreased in stem bases upon fungal infection eight weeks after inoculation, while transcript abundance of two pathogenesis-related (PR) protein isoforms increased significantly, indicating an induced systemic resistance via salicylic acid (Djalali Farahani-Kofoet et al. 2020). Susceptible cultivars obtained an increased resistance after salicylic acid application, indicating a central role of this phytohormone in the systemic acquired resistance towards Fusarium (He and Wolyn 2005).

The impact of Fusarium infection on asparagus root morphology and physiology has been reported, especially with respect to the differential disease severity observed for Fusarium species (Djalali Farahani-Kofoet et al. 2020). However, the systemic response is rather undescribed, while a better understanding for the mechanisms associated with Fusarium infection at the metabolic and proteome level would accelerate the development and selection of cultivars with enhanced resistance. Metabolome analyses can unveil chemical defense strategies of plants and has led to important insights into plant immune responses (Allwood et al. 2021). However, a metabolome analysis of asparagus infected with Fusarium has not been performed so far. Profiling the global proteome during plant-pathogen interaction can potentially identify underlying biosynthetic pathways and identify meaningful markers that can be used for breeding purposes (Ashwin et al. 2017). There is a large knowledge gap for this pathosystem since in the past, only selected defense responses were characterized (Husaini et al. 2018). To better understand the systemic effects of Fusarium infection in asparagus, we have applied a combination of metabolome and proteome analyses, and compared the physiological responses towards the inoculation with *F. oxysporum*, *F. proliferatum* or *F. redolens* in asparagus shoot bases. Dual omics approaches, to simultaneously monitor host and pathogen responses during the infection, have been so far reported for transcriptomic studies on plant-pathogen interactions (Achari et al. 2021; Tu et al. 2023; Bhagat et al. 2024; Zrenner et al. 2020, 2021) and symbiosis (Keller-Pearson et al. 2023), among others. While dual metabolomics is challenging due to the uncertain origin of most metabolites, dual proteomics delivers valuable insights to improve our understanding of pathogenic interactions (Sukumaran et al. 2021). Hence, the interplay of host and pathogen at the protein level was a further focus of this study.

Here, we report on the analysis of the interaction of asparagus with three Fusarium species on the metabolome and proteome level. We specifically chose the stem bases for the analysis as we aimed to identify markers for systemic plant-pathogen interaction. We compared the plant's response to single fungal species infection to unravel species-specific and species-unspecific alterations in the metabolome and proteome.

Materials and methods

Fusarium spp. cultivation

Fusarium spp. isolates used in this study are described in detail previously (Djalali Farahani-Kofoet et al. 2020). Isolates used in the study were *Fusarium oxysporum* f.sp. *asparagi* (Foa 3), *F. proliferatum* (Fpro3) and *F. redolens* (Fred1). The isolates were grown on potato-dextrose agar (PDA; potato dextrose agar, Carl Roth GmbH, Germany) plates. Single spore isolates of each isolate were cultivated on PDA in the dark at 25 °C for 10 days for the studies.

Plant cultivation

Plants were grown as previously described (Djalali Farahani-Kofoet et al. 2020). Briefly, seeds of asparagus (Südwestdeutsche Saatzucht GmbH & Co. KG, Germany) were sown in trays containing a 1:2 mixture of sterilized sand and standardized sterilized plant growth substrate (Fruhstorfer Erde type P, Germany) and cultivated at 25 °C in the dark in a growth chamber until the first stem developed. Plantlets were then exposed to 25/20 °C, 75/85% relative humidity and a 12/12 h day-night-cycle with a light intensity of ca 400 µmol m^{-2} s^{-1} and watered as required. After

development of the third stem, single plants were transferred to pots containing a sterilized 1:1 mixture of sand and standardized plant growth substrate and cultivated at 23/18 °C and 75/85% relative humidity with a 16/8 h photoperiod (ca 400 µmol m^{-2} s^{-1}). Plants were watered three times per week, and after cladode development they were watered twice a week and fertilized once a week with macro- and micronutrients [$Ca(NO_3)_2$ (4.18 g L^{-1}); KNO_3 (1.03 g L^{-1}); KH_2PO_4 (0.35 g L^{-1}); K_2SO_4 (0.43 g L^{-1}); $Mg(NO_3)_2$ (0.51 g L^{-1}); $MgSO_4$ (0.63 g L^{-1}); Fe chelate (0.5 g L^{-1})].

Plant inoculation

Asparagus plants were inoculated as described in detail earlier (Djalali Farahani-Kofoet et al. 2020). In short, plants were carefully removed from the substrate, roots were rinsed with tap water and placed into spore suspensions ($6–8 \times 10^6$ conidia mL^{-1}) for 30 min. Plants were potted into substrate (sand: Fruhstorfer Erde type P, 1:1, vol/vol) and another 9 mL of the spore solution was applied around the stem. Control plants were treated in the same manner but with sterile distilled water. Plants were grown in growth chambers as described above for further 8 weeks. Pots were placed in a randomised complete block design. The experiment was performed three times sequentially. Each experiment included three replications for each isolate and one replicate comprised six plants ($n = 18$). For the detection of fungal DNA in stem bases, three representative plants per treatment and experimental replicate were selected and subjected to the analysis ($n = 9$). For metabolome and proteome analysis, all six plants per treatment and experimental replicate were analysed ($n = 18$).

Fungal DNA detection in stem bases

At the stem basis of each plant a piece of 1 cm of each stem was cut and immediately frozen in liquid nitrogen. Stem pieces were ground in liquid nitrogen in an orbital ball mill for 2 min at a frequency of 30 Hz s^{-1} (MM400 Retsch GmbH, Haan, Germany) with three balls of stainless steel with 5 mm diameter. Total DNA was extracted from at least 50 mg using DNeasy Plant Mini Kit (Qiagen GmbH, Hilden, Germany) and quantified spectrophotometrically (Infinite M200PRO, Tecan Trading AG, Switzerland) using the NanoQuant plate. Quality was checked using an absorption ratio of 260 nm to 280 nm of > 1.8. Fungal DNA standard curves were performed with mycelium harvested from single spore isolates grown for 5 days in liquid culture in potato dextrose medium in the dark at 25 °C using the same method. A serial dilution of samples of 2.5–0.001 ng of fungal DNA with and without 20 ng of pure *A. officinalis* genomic was used for the standard curves. For qPCR primer concentrations of 200 nM and 3 µL of extracted DNA solution were used in each reaction in 10 µL with the Sensi Fast SYBR NO ROX Kit (Bioline GmbH, Luckenwalde, Germany). The qPCR cycling was as follows: 95 °C for 5 min to activate the polymerase, 40 amplification cycles of 95 °C for 15 s and 60 °C for 1 min with signal thresholds set automatically. Primers were based on sequence variations previously analyzed (Mulè et al. 2004b, 2004a; Borrego-Benjumea et al. 2014): *F. oxysporum* f.sp. *asparagi*, Fo-RT-CL1f1: TTCATTTCTGCTGCTGAGCTTC, FoCL1r: GTCAGTAACTGGACGTTGGTACT; *F. proliferatum*, FpCL1f: CATGCATCAGACCAC TCAAATC, Fp-RT-CL1r1: CGTTTAGCTCATGTT TTCGCTTC; *F. redolens*, FrEF1f: ATTTTCCCT TCGACTCGCCG, Fr-RT-EF1r2: GATCCGCGC TCATTGTGATTG.

Metabolite extraction from stem bases

A 1 cm piece of each stem was cut directly at the stem basis of each plant for metabolite analysis. Samples were immediately frozen in liquid nitrogen and stored at -80 °C. Samples were taken from three representative plants of each treatment per replicate and experiment. Plant material was ground in liquid nitrogen in an orbital ball mill for 2 min at a frequency of 30 Hz s^{-1} (MM400 Retsch GmbH, Germany) with three balls of stainless steel with 5 mm diameter. The fresh weight was taken and the homogenized material was extracted in 4 mL of acetonitrile/methanol/water (16:3:1, vol/vol/vol) + 0.1% formic acid. After 5 min incubation in ultrasonic bath, samples were centrifuged for 20 min and the supernatant was transferred into a new tube. The pellet was extracted two times more with 2 mL extraction solution, each. All supernatants were collected and concentrated to dryness (Concentrator 5301, Eppendorf, Germany).

Metabolite analysis of stem bases

The samples were redissolved in acetonitrile/water (5/95, v/v) + 0.1% formic acid (LC–MS grade, Fisher Scientific and Merck, Germany) to result in a stem concentration of 0.5 g/mL using an ultrasonic bath (5 min). The samples were then centrifuged for 5 min at 15.000 × *g* and filled into LC vials prior to injection.

HPLC-ESI-QTOF-HRMS measurements were based on Döll et al. (2021) with several modifications: chromatographic separations were performed on an Elute HPG 1300 UHPLC system having an Elute column oven (Bruker Daltonics, Germany) and being equipped with a PAL HTC-xt autosampler (CTC Analytics AG, Switzerland). Chromatographic separation was performed at 40 °C on a Nucleodur C18 Gravity-SB column (75 × 2 mm, 1.8 µm, Macherey–Nagel GmbH & Co. KG, Germany) equipped with a KrudKatcher Ultra (Phenomenex, Germany). Gradient elution conditions using acetonitrile + 0.1% formic acid (A) and water + 0.1% formic acid (B) were applied as follows: 0.0 min 5% A, 2.0 min 5% A, 3.9 min 25% A, 6.5 min 70% A, 7.5 min 70% A, 9.0 min 95% A, 12.0 min 95% A, 12.2 min 5% A, and 15.0 min 5% A. Additionally, a flow gradient of 350 µL/min respective 450 µL/min (3.9–12.2 min) was included. The first 2 min of each run were directed into waste. The software Compass HyStar (versions 5.10) (Bruker Daltonics, Germany) was used for the operation of the UHPLC system. The injection volume was 30 µL. Eluted compounds were detected from m/z 90 to 1600 at a spectrum rate of 4 Hz, (line and profile spectra) using an Impact II QTOF mass spectrometer equipped with an Apollo II ESI source (Bruker Daltonics, Germany). The parameters for the Apollo II source were set as follows: ionization was performed in the positive and negative mode at 4.5 and − 3.0 kV, respectively. Dry gas temperature was set to 220 °C at a flow rate of 10.0 L/min. Nebulizer gas pressure was 2 bar. Further instrument settings were: end plate offset, 500 V; funnel 1 radio frequency (RF), 100 Volts peak-to-peak (Vpp); funnel 2 RF, 200 Vpp; in-source collision-induced dissociation (CID) energy, 0 eV; hexapole RF, 50 Vpp; quadrupole ion energy, 4 eV; quadrupole low mass, 90 m/*z*; collision energy, 10 eV (positive ionization mode), 7 eV (negative ionization mode); prepulse storage, 10 µs. Stepping: on; basic mode; collision cell RF, from 250 to 1000 Vpp; transfer time, from 25 µs to 90 µs; 50%/50%, collision energy for MSMS, 80–120%.

Fragmentation took place in a collision-induced dissociation cell using nitrogen. For the acquisition of CID (collision induced dissociation) mass spectra, the same parameters as above were used with additional settings for data dependent acquisition (AutoMSMS): Mode: CID, intensity threshold 600, number of precursors, 3, active exclusion on after 3 spectra, release after 1 min, smart exclusion, on, 5x; isolation and fragmentation settings, size and charge dependent, width 3–15 m/z, collision energy 10–70 eV, charge states included: 1z, 2z, 3z. Sodium formate cluster ions were applied for instrument mass calibration and for re-calibration of individual raw data files. The software Compass Control (software versions 4.1, Bruker Daltonics, Germany) was used for the operation of the mass spectrometer and for data acquisition.

The re-calibrated LC-QTOF-MS raw data was processed with Bruker Compass MetaboScape Mass Spectrometry Software, Version 2022b (Bruker Daltonik GmbH, Bremen, Germany). Mass recalibration, peak picking, peak alignment, region complete feature extraction, and grouping of isotopes, adduct and charge states were performed with the T-ReX algorithm in MetaboScape. The settings were as follows: Peak detection: Intensity threshold: 1500 counts, minimum peak length: 8 spectra, feature signal: intensity, minimum peak length for recursive feature extraction: 7 spectra, retention time range: 2–15 min, mass range: 90–1600 m/z, MSMS import method: average, grouped by collision energy, ion deconvolution: EIC correlation = 0.8, primary ion: $[M+H]^+$, seed ions: $[M+Na]^+$, $[M+K]^+$, common ions: $[M+H\text{-}H_2O]^+$, T-ReX Positive Recalibration: Auto-Detect. With these settings, a feature table of 17793 features was created. Features from blanks were excluded when the maximum signal in samples divided by maximum signal in blanks was ≤ 3. Further, 2426 features that were also present in blanks were excluded from the analysis.

For compound annotation, first, all fragment spectra were matched against an in-house library containing the mass retention time and spectra of 500 commercial standards of plant metabolites using MetaboScape's target list search. Second, the mycotoxins that were already measured individually by authentic standards were manually identified in the

data set. Third, all fragment spectra were matched in a parallel search against the following spectral data bases: NIST17 (The NIST Mass Spectrometry Data Center, U.S. Department of Commerce, Gaithersburg, MD, USA), and the following databases downloaded from MoNa—Mass Bank of North America (https://mona.fiehnlab.ucdavis.edu/downloads): LipidBlast 2022 (Kind et al. 2013), Fiehn-Hilic, ReSpect (Sawada et al. 2012), GNPS (https://gnps.ucsd.edu/), Vaniya-Fiehn Natural Products and MoNa MassBank (https://mona.fiehnlab.ucdavis.edu/) (Kind et al. 2009), using the MetaboScape Spectral Library Search function (Parameters: Filter: exact match of data base entry to precursor mass. Tolerances (narrow-wide): m/z 2-10mDa, mSigma 20–100, MS/MS score 900–750). Results from the analyte list and the spectral library search can be found in the feature table column "name". The second approach for annotation used the SIRIUS Software version 5.8.0 (Dührkop et al. 2021, 2019; Feunang et al. 2016; Kim et al. 2021). Sirius combines sum formula generation using exact mass and isotope pattern with the fragmentation patterns of MS/MS spectra. De novo compound class prediction is achieved with the CANOPUS module. The settings for SIRIUS were as follows: Instrument: Q-ToF, Filter by isotope pattern, ignore isotope scorer, candidates stored: 1, minimum candidates per ion stored: 1, tree timeout: 0, compound timeout: 0, use heuristic above m/z 300, use heuristic only above m/z 650. Possible ionizations: $[M+H]^+$, $[M+K]^+$, $[M+Na]^+$. Allowed elements: H (0-inf.), C (0-inf), N (0–12), O (0-inf), P (0–6), S (0–6).

Protein extraction from stem bases and proteome analysis

Stem bases were sampled and the material was homogenized as described above for metabolite analysis. Proteins were extracted from 100 mg using RapiGest SF (Waters, Germany). Ten µg of protein were reduced, alkylated and digested with trypsin over night at 37 °C. Desalting of peptides was carried out using peptide desalting spin columns (Pierce, Thermo Scientific, United States) following the manufacturer's instructions. Peptide concentration was adjusted to 100 ng/µL and 6 µL of protein digest were analyzed using nanoflow liquid chromatography on a Dionex UltiMate 3000 system (Thermo Scientific) coupled to a Q Exactive Plus mass spectrometer (Thermo Scientific). Peptides were separated using an Acclaim PepMap 100 C18 analytical column (75 µm × 50 cm, 2 µm, 100 Å, Thermo Scientific) and eluted via a 200 min gradient from 2 to 44% solvent B (80% acetonitrile in water with 0.1% formic acid), with solvent A being 0.1% formic acid in water, with the column temperature set at 40 °C. For electrospray ionization of peptides, a Nanospray Flex ion source was used, with spray voltage set at 1.80 kV, capillary temperature at 275 °C, and S-lens RF level at 60. Mass spectra were acquired in positive ion and data-dependent mode. Full-scan spectra (375 to 1,500 m/z) were acquired at 140,000 resolution and MS/MS scans (200 to 2,000 m/z) were conducted at 17,500 resolution. Maximum ion injection time was 50 ms for both scan types. The 20 most intense MS ions were selected for collision-induced dissociation fragmentation. Singly charged ions and unassigned charge states were rejected; dynamic exclusion duration was set to 45 s.

The raw files were processed using Proteome Discoverer 2.4 and Sequest HT engine (Thermo Scientific), searching either the NCBI *A. officinalis* Annotation Release 100 (as released on 1 March 2017), the *F. oxysporum* NCBI RefSeq assembly GCF_013085055.1, the *F. proliferatum* NCBI RefSeq assembly GCF_900067095.1 or the *F. redolens* NCBI RefSeq assembly GCF_020744475.1. Precursor ion mass tolerance was set to 10 ppm and fragment ion mass tolerance was set to 0.02 Da. False discovery rate (FDR) target values for the decoy database search of peptides and proteins were set to 0.01 (strict level for highly confident identifications). Protein abundance quantification was carried out using the Top N average method ($n = 3$) on proteins that were detected in at least 50% of runs in the replicate group. Differential protein expression was validated using t-test ($p < 0.05$, Benjamini–Hochberg corrected for FDR), after an analysis of variance (ANOVA) test, implemented in the Proteome Discoverer software (Thermo Scientific). The result lists were filtered and proteins were only kept for further investigation if: identified by at least two peptides or by one peptide representing at least 10% protein coverage. Functional annotation of proteins was performed using BlastKOALA and the Kyoto Encyclopedia of Genes and Genomes (KEGG) pathway database (Kanehisa et al. 2016). Functional analysis of differential expressed proteins was performed using both MapMan (Usadel

et al. 2009) annotated with Mercator (Lohse et al. 2014) and g:Profiler (Kolberg et al. 2023). For MapMan analysis the *A. officinalis* uniprot proteome UP000243459_4686.fasta file was annotated using the Mercator pipeline, imported into the MapMan platform, together with the log2 transformed protein abundance ratios of the validated differential protein expression. For g:Profiler analysis the detected asparagus protein accessions were linked to the respective locus tags on the asparagus genome assembly Aspof. V1 (NCBI RefSeq assembly GCF_001876935.1) and these were used in g:Profiler analysis. For the g:Profiler analysis of the detected Fusarium proteins the Fusarium protein accessions were linked to the respective *F. oxysporum* f. sp. *lycopersici* 4287 (NCBI ASM14995v2 RefSeq assembly GCF_000149955.1) gene ID to be used in the gProfiler analysis.

Data analysis

Venn diagrams of metabolite and proteome data were created using BioVenn (Hulsen et al. 2008). Box plots and non-parametric tests shown within were created with Sigma Plot 14.0 (Systat Software, Germany). Voronoi treemaps were generated using SRplot (http://www.bioinformatics.com.cn/srplot).

Results

Colonization pattern of *Fusarium* spp. in asparagus

Previously, we have tested the Fusarium species-specific disease severity on asparagus. Typical disease symptoms were a reduced root and fern fresh weight, development of brown to reddish-brown necrotic spots on roots and lesions of variable length on storage and fibrous roots (Djalali Farahani-Kofoet et al. 2020). The most aggressive isolates for the present study were *F. proliferatum* Fpro3 and *F. redolens* Fred1, where phenotypes were more severe than *F. oxysporum* Foa3 infection symptoms, resulting in degraded parenchyma tissue of roots and strong degradation of fibrous roots (Fig. 1A). Concomitant to the disease symptoms on roots, fungal DNA was detected in stem bases of infected plants, indicating

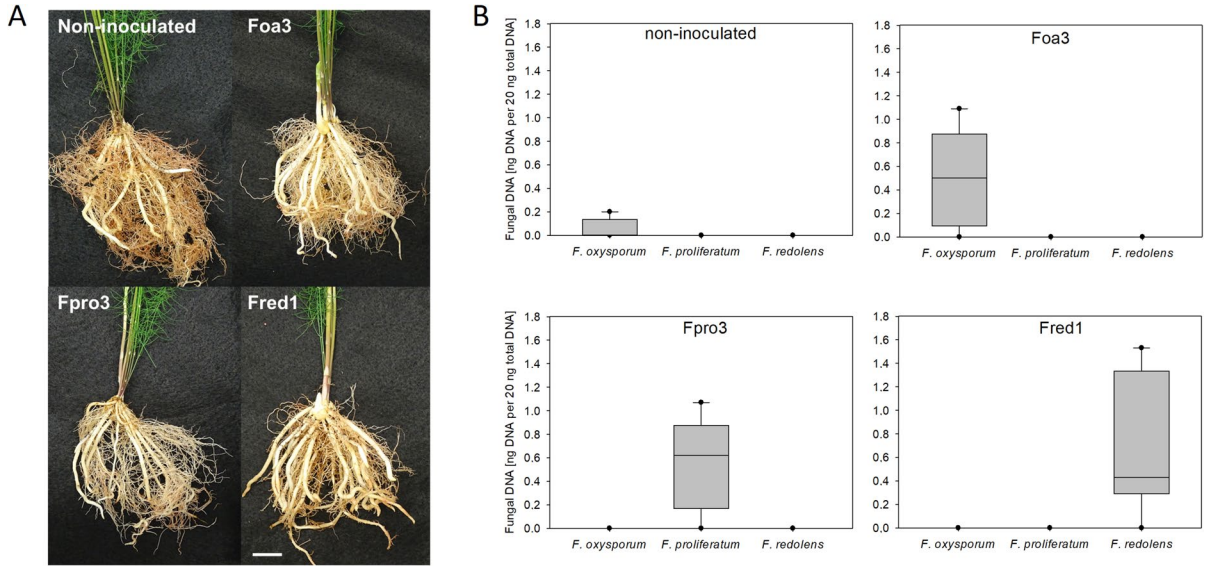


Fig. 1 Root disease symptoms and systemic spread of Fusarium species in asparagus cv. Backlim. **A** Roots were inoculated with *F. oxysporum* Foa3, *F. proliferatum* Fpro3 or *F. redolens* Fred1 and show a strong degradation of fibrous roots, while storage roots largely remain intact eight weeks after inoculation, when compared to the non-inoculated control. **B** Detection of fungal DNA in stem bases of non-inoculated and inoculated asparagus plants. Box plots show the amount of fungal DNA in basal shoots, based on all replicate experiments (three experiments with three plants each, $n=9$) as detected with qPCR. All samples were analyzed with primer pairs specific to the three Fusarium species. The median, 5th and 95th percentiles are plotted as vertical boxes with error bars

a progressed colonization of host plants. Quantitative PCR using species-specific primer pairs revealed the presence of *F. oxysporum*, *F. proliferatum* and *F. redolens* in plants inoculated with the respective isolates solely (Fig. 1B). In non-inoculated plants, low DNA amounts of *F. oxysporum* were detected, indicating latent colonization of plants with potentially nonpathogenic *F. oxysporum* strains, which caused no disease symptoms. All DNA quantifications showed a high variation among individual plant samples, indicated by the size of error bars, which reflects the typical non-uniform disease progression in adult plants.

Fusarium infection reduces fatty acid-related compounds in asparagus stem bases

A better understanding of the metabolic regulation of Fusarium infection is a prerequisite for developing strategies for disease control. Measurements of stem bases from infected and non-infected plants by positive ion electrospray ionization (ESI^+) led to the detection of 18,690 mass/retention time pairs. Principal component analysis revealed a distinct separation between metabolomes of non-infected and infected plants, while metabolite profiles of plants infected with one of the three Fusarium species did not reveal a clear species-specific effect (Supplemental Fig. 1A). A paired t-test ($p > 0.05$) was performed to identify features that significantly changed in their abundance upon infection when compared to the control samples. A total of 7,418 ESI^+ signals significantly differed between control and Foa3 samples, while 9,045 and 9,076 features differed between control and Fpro3 and Fred1 samples, respectively. To analyze the species-specific and species-unspecific effect on the metabolome, the distribution of features was visualized using Venn diagram (Supplemental Fig. 1B) and showed that the highest species-specific impact on the asparagus metabolome was induced by Fred1 infection, followed by Fpro3 and Foa1. Overall, the response of the metabolome towards Fusarium infection was relatively species-unspecific since the majority of differential abundant metabolites was shared by all three isolates.

Database-driven annotation was successful for 421 compounds and compound class prediction using Canopus Natural Product Classifier was achieved for 387 compounds. Whether those features derive from the plant or from the fungal pathogen cannot be fully clarified. A number of fungal mycotoxins, such as FB1, FB2 and FB4, BEA, ENN A, ENN A1 and ENN B1 were detected (Fig. 2). Plants inoculated with Foa3 accumulated mainly BEA as well as lower amounts of fumonisins. Only FB1, FB2 and FB4 were detected in stem bases of Fpro3 inoculated plants, while a complex mixture of ENN A, ENN A1, ENN B1, and traces of BEA and FB1 was found in samples from Fred1 inoculated plants. Traces of BEA were also detected in non-inoculated plants, which corresponds to the low level of *F. oxysporum* DNA detected in those plants. Moniliformin, a frequently produced mycotoxin in Fusarium species, could not be quantified.

From all annotated compounds, 124 were significantly changed in abundance in plants infected with Foa3, with 75% of them being lower abundant as compared to the control. 157 compounds were detected as differential abundant in response to Fpro3 infection and also here, the majority of compounds was lower abundant in samples from infected plants as compared to the control (73%). Similarly, 166 compounds were differential abundant in Fred1 infected plants and from those, 60% were lower abundant in the infected stem bases. From those three comparisons, 93 compounds were found to be significantly changed in abundance by all three Fusarium isolates and the direction of change (more abundant vs. lower abundant as compared to the control) was the same for all metabolites, indicating a general Fusarium species-unspecific impact on the asparagus stem base metabolome, except for two compounds annotated as avenobenzone and 1-naphthaldehyde (Supplemental Table 1). Compound class prediction and subsequent visualization using Voronoi treemaps revealed that the main pathway affected by Fusarium infections was “Fatty acids” with 117 unique compounds falling into this category, specifically the superclasses “Glycerophospholipids”, “Glycerolipids” and “Sphingolipids” (Fig. 3), being lower abundant in infected plants (Fig. 4). This indicates that not only sphingolipid- and lipid-based signaling processes are negatively affected by the fungal pathogens, but also fundamental processes such as vesicle formation, membrane integrity and cell wall organization.

Another main pathway identified in the analysis was “Shikimates and Phenylpropanoids”, consisting of the superclasses “Flavonoids”, “Coumarins”

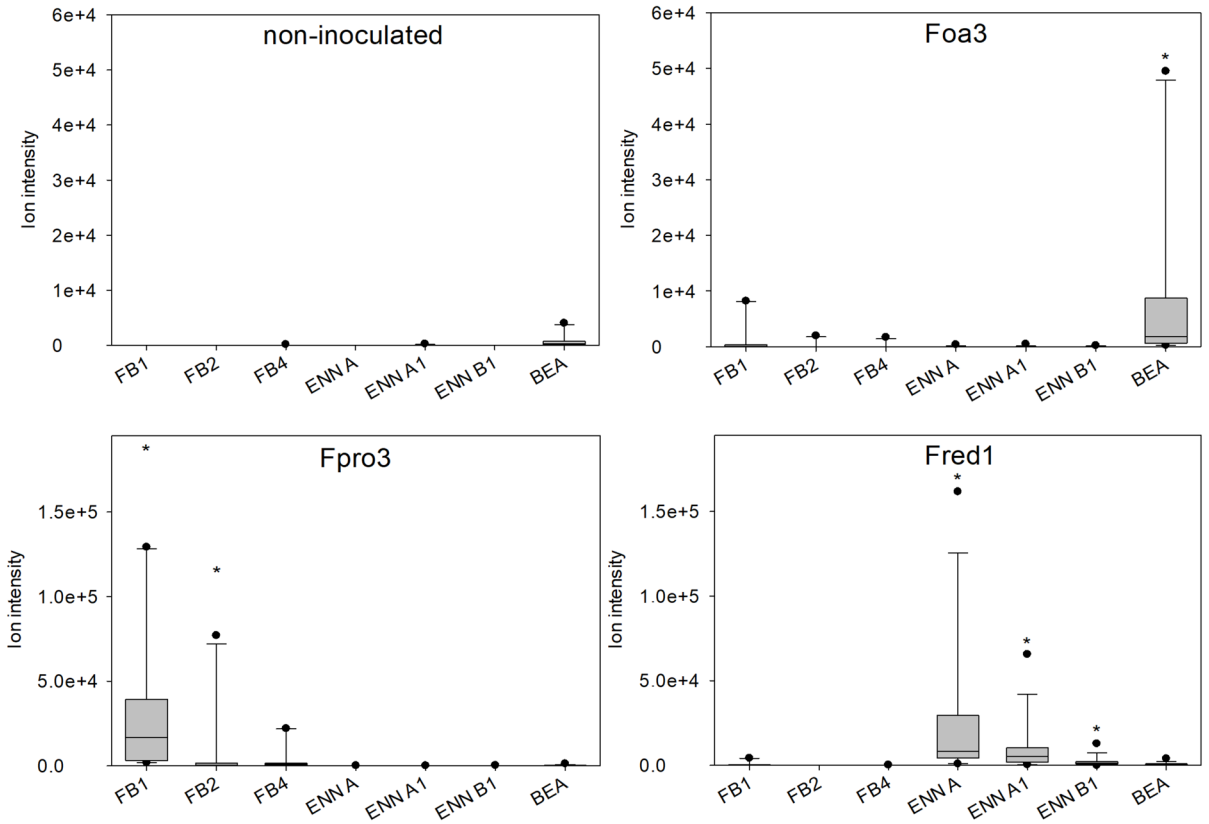


Fig. 2 Detection of mycotoxins (fumonisins: FB1, FB2, FB4; enniatins: ENN A, ENN A1, ENN B1; beauvericin BEA) in stem bases of asparagus inoculated with Foa3, Fpro3, Fred1 or the non-inoculated control. Box plots show the abundance of selected compounds, based on all replicate experiments (three experiments with 9 plants each, $n = 18$). The median, 5th and 95th percentiles are plotted as vertical boxes with error bars. Asterisks (*) indicate significant differences between the non-inoculated control plants and plants inoculated with the respective Fusarium isolate (t-test, $p < 0.05$)

and "Phenylpropanoids", among others. Here, abundance was differential with some compounds being induced by the infections, such as chelidonic acid, esculin, 8-acetyl-7-methoxycoumarin, kaempferol-3-O-glc-1–3-rham-1–6-glucoside and 2,3-dihydroxybenzoic acid (Supplemental Fig. 2), while others were depleted in infected plants, such as syringic acid. 2,3-dihydroxybenzoic acid is a product of salicylic acid catabolism and while salicylic acid did not accumulate in infected stem bases, we found higher levels of this inactive form in plants inoculated with Fusarium species, especially by Fred1 (Supplemental Fig. 3). In general, more compounds in this pathway were induced by Fred1 infection (24 compounds) as compared to Foa3 (7 compounds) or Fpro3 (12 compounds) infection, when related to non-inoculated plants.

Differential abundance of plant proteins involved in defense responses and membrane trafficking upon Fusarium infection

The proteome alterations in asparagus stem bases in response to Fusarium infection were investigated using a label-free LC–MS approach. The analysis resulted in 1.193.929 peptide spectrum matches, indicating 25.116 peptides and 4,818 proteins when using the asparagus protein database. Principal component analysis revealed a clear separation between inoculated and non-inoculated samples, and a distinct separation of Foa3 inoculated samples (Supplemental Fig. 4A). The data set was filtered according to the parameters described in the Materials and Methods section and 3,610 identified proteins were subjected

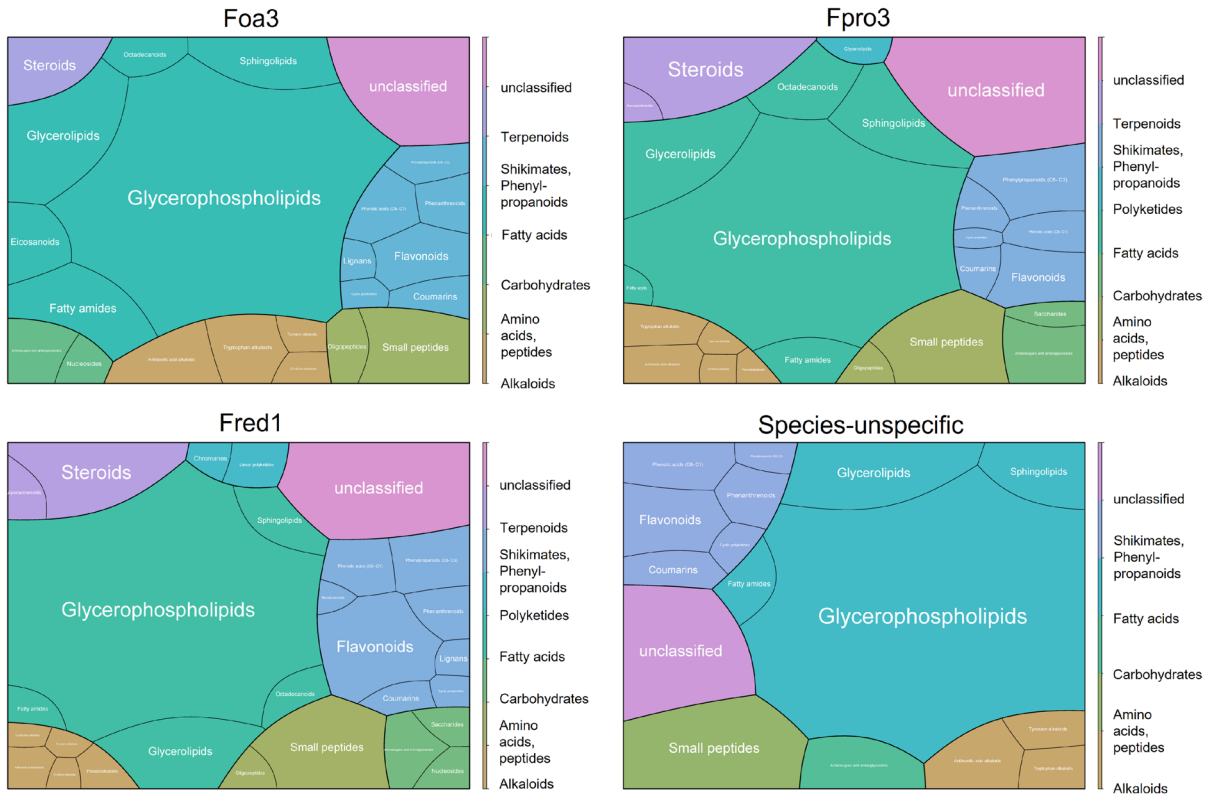


Fig. 3 Voronoi treemaps visualizing changes in the metabolite abundance with respect to Fusarium infection. Functional annotation of compounds was based on Canopus compound class prediction tool. Overall, 124 compounds were specifically altered in plants infected with Foa3, while 157 and 166 compounds were detected as significantly differentially abundant in plants infected with Fpro3 or Fred1, respectively. Out of these compounds, a significantly changed abundance of 93 compounds was found in response to Fusarium infection, irrespective of the isolate. Compound IDs, full Canopus Natural Product Compound annotation and abundance ratios are provided in Supplemental Table 1

to statistical analysis (paired t-test, $p > 0.05$). To analyze the species-specific and species-unspecific effect on the proteome, the distribution of proteomes was visualized using Venn diagram (Supplemental Fig. 4B) and showed that the highest species-specific impact on the asparagus proteome was induced by Foa3 infection, followed by Fred 1 and Fpro3. Overall, the response of the proteome towards Fusarium infection showed a higher species-specificity as compared to the metabolome alterations in response to infections, probably due to the occurrence of multiple protein isoforms leading to the same physiological response.

Since the metabolome analysis revealed a decreased abundance of salicylic acid and increased abundance of its inactive form 2,3-dihydroxybenzoic acid in all infected stem bases, the proteome data set was investigated for the abundance of pathogen defense-related proteins. In total, 68 proteins were identified that functionally belong to PR proteins, proteinase inhibitors, subtilisin-like proteases, mitogen-activated protein kinases, among others. Differential abundance in response to Fusarium inoculation was found for 35 of those proteins and the expression pattern was rather species-specific (Fig. 5). For example, inoculation with Foa3 led to a strong induction of a Bowman-Birk type proteinase inhibitor D-II-like protein (gi:1150729583), a germin-like protein subfamily 2 member 4 (gi:1150707065) and a stress-induced protein C29B12.11c (gi:1150747261) in stem bases. Inoculation with Fpro3 and Fred1 revealed a more similar expression pattern with a strong induction of a pathogenesis-related protein 1-like protein (gi:1150709591), a second pathogenesis-related

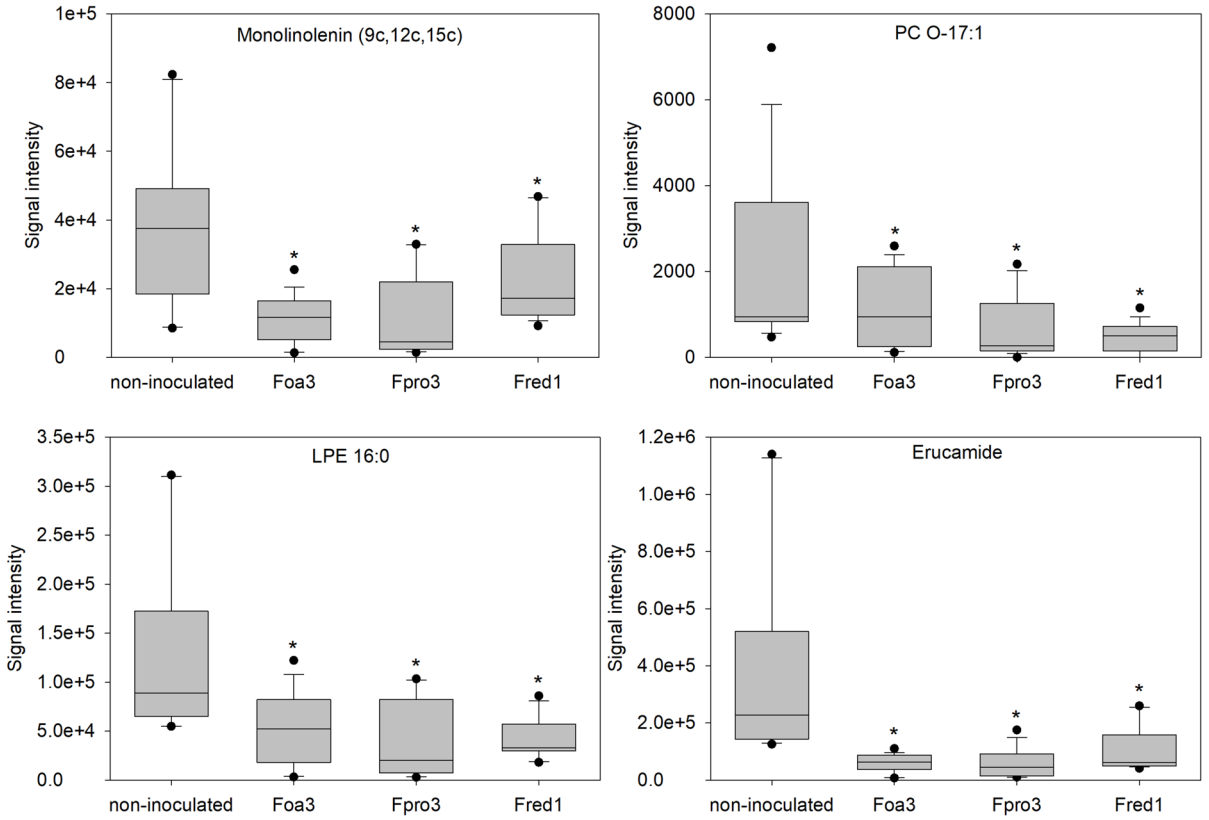


Fig. 4 Detection of "Fatty acids"-related metabolites in stem bases of asparagus inoculated with Foa3, Fpro3, Fred1 or the non-inoculated control. Box plots show the abundance, based on all replicate experiments (three experiments with 9 plants each, $n = 18$). The median, 5th and 95th percentiles are plotted as vertical boxes with error bars. Asterisks (*) indicate significant differences between the non-inoculated control plants and plants inoculated with the respective Fusarium isolate (t-test, $p < 0.05$). Four compounds were selected exemplary for different CANOPUS Natural Compound Classes: monolinolenin (9c,12c,15c) for glycerolipids (monoacylglycerols), PC O-17:1 [1-(10Z-heptadecenoyl)-2-hydroxy-sn-glycero-3-phosphocholine] for glycerophospholipids (glycerophosphocholines), LPE 16:0 ([(2*R*)-1-[2-aminoethoxy(hydroxy)phosphoryl]oxy-3-hydroxypropan-2-yl] hexadecanoate) for glycerophospholipids (glycerophsophoethanolamines) and erucamide ((*Z*)-docos-13-enamide) for fatty amides (N-acyl amines)

protein 1-like protein (gi:1150731607) as well as de novo synthesis of a mitogen-activated protein kinase homolog MMK2-like protein (gi:1150702216) and subtilisin-like protease SBT1.2 (gi:1150720322) and subtilisin-like protease SBT1.7 (gi:1150737390). Additionally, Fred1-inoculated samples showed a highly increased abundance of thaumatin-like protein (gi:1150690425) and de novo synthesis of pathogenesis-related protein PRB1-3-like protein (gi:1150690709). Further, three proteins of the nuclear transcription factor Y subunit family (gi:1150736044, gi:1150676848, gi:1150672787) were found exclusively in inoculated plants.

The metabolome analysis also revealed an accumulation of specific compounds involved in the plant's response to pathogen attack, such as shikimates and phenylpropanoids. Hence, the proteome data set was investigated for the abundance of proteins involved in their biosynthetic pathways. However, we did not find a clear induction of biosynthetic pathways in the infected plants. This is probably due to the fact that samples for metabolome and proteome analysis were taken at the same time. In order to analyze early steps in the biosynthetic pathways, an earlier sampling timepoint for proteome analysis would give more information.

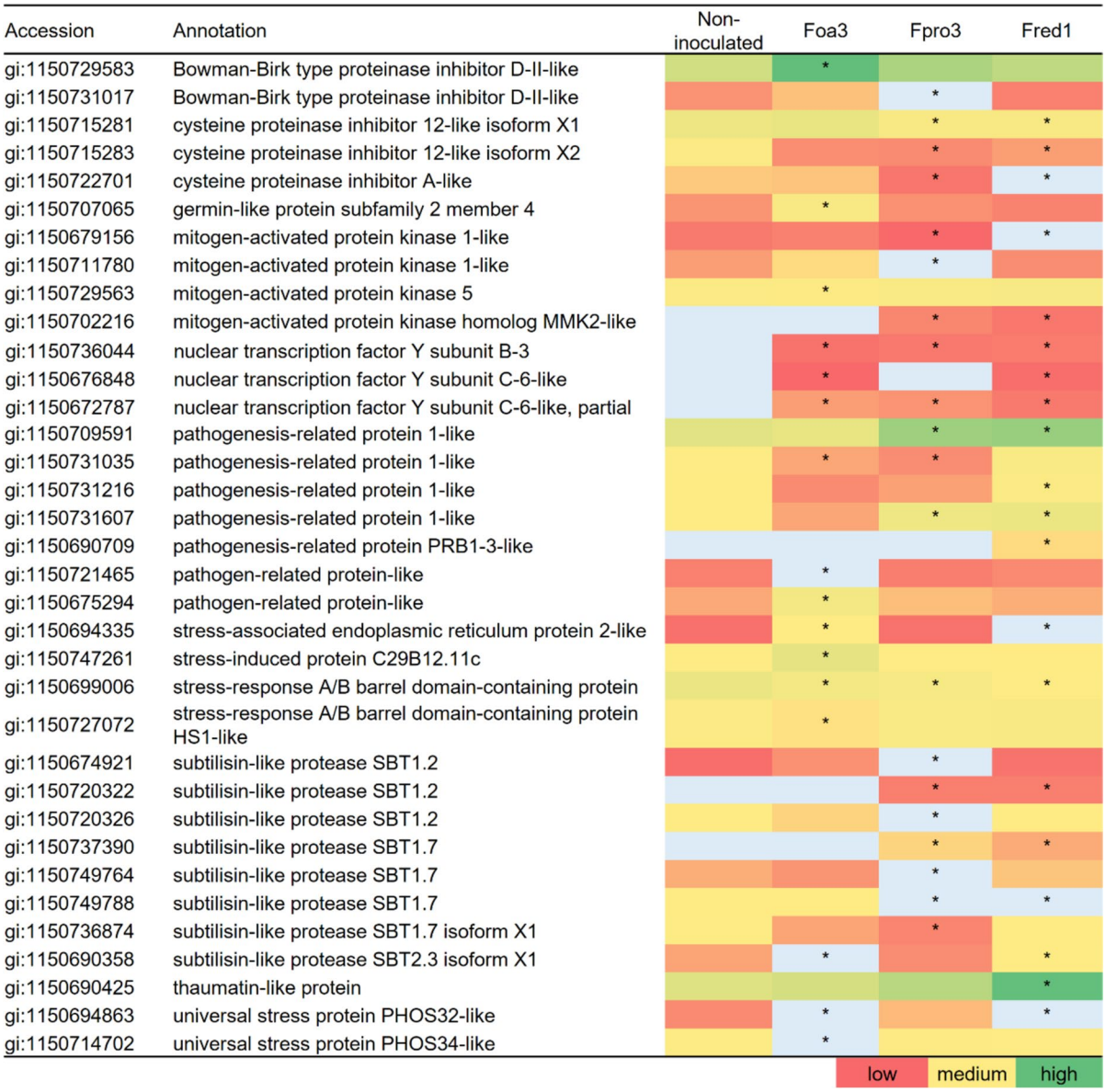


Fig. 5 Heatmap depicting proteins that were identified by the proteome analysis as involved in pathogen defense-related responses. Colors represent the normalized protein expression ranging from minimum (dark red, 4.5E5 ion intensity) via medium (yellow, 8.8E6 ion intensity) to maximum (dark green, 2.2E8 ion intensity). Grey color indicates the absence of the protein in the respective group. Asterisks (*) indicate significantly different protein abundances (t-test, $p < 0.05$) between non-inoculated and respective inoculated samples. Further information related to protein accession numbers, abundance ratio, and significance testing is provided in Supplemental Table 2

However, we found an induction of cytochrome P450 proteins, a group of proteins involved in hormone signaling and plant defense (Pandian et al. 2020). A total of 13 cytochrome P450 proteins were identified in the proteome data set and out of those, six proteins were higher abundant or exclusively expressed in inoculated stem bases (Supplemental Fig. 5).

A comprehensive functional annotation of all changes in protein abundance with respect to *Fusarium* infection was done using the tools MapMan and gProfiler. 702 proteins were specifically altered in

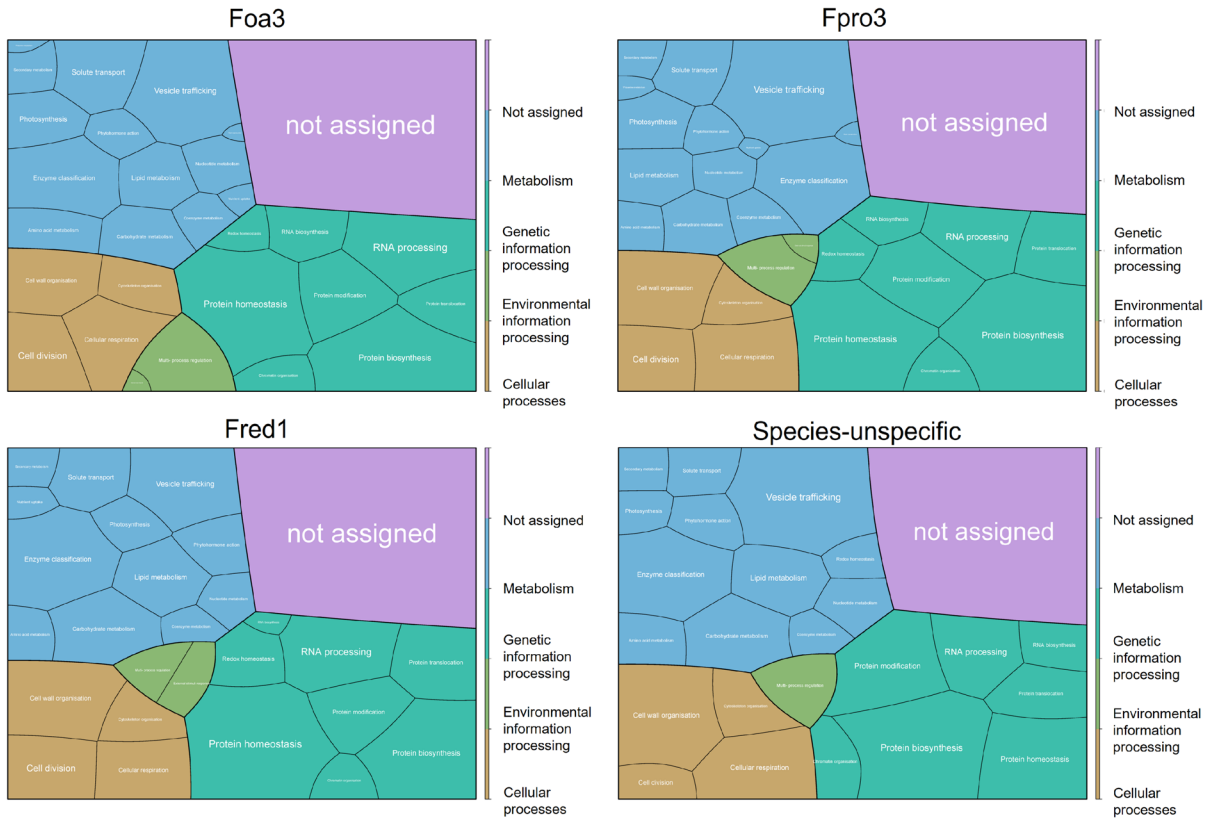


Fig. 6 Voronoi treemaps visualizing changes in the protein abundance with respect to Fusarium infection. Functional annotation was based on MapMan tool. 702 proteins were specifically altered in plants infected with Foa3, while 500 and 565 proteins were detected as significantly differentially abundant in plants infected with Fpro3 or Fred1, respectively. Among those, a significantly changed abundance of 150 proteins was found in response to Fusarium infection, irrespective of the isolate. Protein identifications, full Gene Ontology annotation and abundance ratios are provided in Supplemental Table 2

plants infected with Foa3, while 500 and 565 proteins were detected as significantly differentially abundant in plants infected with Fpro3 or Fred1, respectively. From those three comparisons, 150 proteins found to be significantly changed in abundance by all three *Fusarium* isolates, while the highest impact on the asparagus proteome was induced by Foa3 infection (702), followed by Fred1 (565) and Fpro3 (500), as visualized by Voronoi treemaps (Fig. 6). Protein identifications, MapMan annotation, gProfiler analysis and abundance ratios are provided in Supplemental Table 2. For testing of statistical significance in functional enrichment analysis, the gProfiler tool was applied and confirmed the non-specific response of asparagus to the Fusarium-isolates. So-called driver terms, which are leading protein sets in the enrichment analysis, with respect to biological function were identified in Foa3-infected plants as "biological_process" (GO:0008150), "RNA splicing" (GO:0008380, increased protein abundance) and "proton transmembrane transport" (GO:1902600, decreased protein abundance), overlapping with both, Fpro3- and Fred1-infected plants, that showed "biological_process" (GO:0008150) and "proton transmembrane transport" (GO:1902600) as driver terms. Impairment in proton transmembrane processes likely favors Fusarium proliferation in infected tissues since the extracellular alkalinization provoked by the pathogen is a prerequisite for hyphal growth and a main pathogenicity factor (Mariscal et al. 2022).

MapMan analysis revealed that "Vesicle trafficking" is the superior bin commonly altered upon inoculation with the different *Fusarium* spp. This clearly indicates the role of the movement of enzymes,

biochemicals or signaling molecules in the interaction between host and pathogen. This is further visualized by the heatmap depicting proteins involved in vesicle trafficking processes (Supplemental Fig. 6). While some of the altered protein abundances are common between inoculations with the three different Fusarium species [GTP-binding protein SAR1A-like isoformX1 (gi:1150725539), IST1-like protein (gi:1150681415), alpha-soluble NSF attachment protein-like (gi:1150699389), or ras-related protein Rab7 (gi:1150677177)], others showing a rather species specific alteration pattern [e.g. exocyst complex component SEC8 isoform X1 (gi:1150726733), or DENN domain and WD repeat-containing protein SCD1 (gi:1150711736)]. Further enriched MapMan bins are "Redox homeostasis" in Fpro3 infected plants, "Cell wall organization" and "Multi-process regulation" in Fred1 infected plants, while "Cell division" is enriched exclusively in Foa3 infected plants (Supplemental Table 2). These are all fundamental processes specifically known as being associated with infection and pathogen control.

Proteins involved in vesicle transport processes were assessed further in detail, since vesicle formation is essential for mycotoxin sequestration in vacuoles, inter- and intracellular transport processes as well as deposition of extracellular material as defense response (Wang et al. 2021; Wang and Dong 2011). A total of 70 proteins were found differential abundant between the non-inoculated control and plants inoculated with one of the three Fusarium isolates with the majority either being downregulated or absent in response to fungal infection (Supplemental Fig. 6). Proteins in the largest group with 27 proteins were involved in trafficking regulation, such as vesicle tethering and target membrane fusion, indicating that mediating the attachment of specific transport vesicles to their destination membranes as well as the subsequent membrane fusion is impaired upon fungal infection. The second largest group consisted of 19 proteins and those were involved in retrograde trafficking from Golgi apparatus or the vacuole to the endoplasmic reticulum (ER), which could point to a disturbed endomembrane system. Remaining proteins were involved in endocytosis, secretory pathways as well as anterograde trafficking, indicating a vast reprogramming of host membrane trafficking by the fungal pathogen.

Detection of fungal virulence proteins in infected stem bases

Proteome raw data was also subjected to a database search using available reference genome sequences of *F. oxysporum*, *F. proliferatum* and *F. redolens*. On average, 102 proteins were detected in plants infected with Foa3, while 22 and 23 proteins were detected in plants infected with Fpro3 and Fred1, respectively. In non-inoculated plants, 26 fungal proteins were found. Due to the high variation in fungal protein amounts in the individual plants, as also verified by fungal DNA quantification (see Fig. 1), a direct proteome comparison between groups was not possible. Instead, proteins that were found in at least 50% of all replicates in one treatment group and revealed a high similarity of the fungal protein complement within asparagus stem bases were compared. Proteins found in plants infected with all three Fusarium species included actin, adenosylhomocysteinase, ADP-ribosylation factor, ubiquitin-related proteins, proteins involved in protein biosynthesis and membrane trafficking (Supplemental Table 3).

Since the highest number of fungal proteins was detected in plants inoculated with Foa3, this dataset was investigated in more detail. In total, 1,488 unique *F. oxysporum* proteins were detected in asparagus stem bases. A gProfiler analysis revealed an enrichment in proteins that are involved in "ribonucleotide binding" and driver terms like "ATP and GTP dependent activities" were enriched. But also "fatty acid biosynthetic process", "protein containing complex" or "cytoskeletal motor activity" were significantly found (Supplemental Table 3). This all indicates that at least Foa3 can thrive in the asparagus plants. The dataset was further investigated for the presence of known virulence factors. Two members of the SIX ('Secreted in Xylem') protein family were found: XP_031031589.2 and XP_054561445.1, which are effector proteins, as well as pectate and pectin lyases (XP_031044270.2, XP_059465782.1, XP_031043893.1) involved in cell wall degradation. A Cerato-platanin-domain-containing protein (XP_031030973.2) was detected that probably can induce plant defense responses, such as hypersensitive response or cell death. Two catalase-peroxidases (XP_031030333.2, XP_031029925.2) that act in protecting the pathogen from high H_2O_2 levels produced by the plant. Ribonuclease/ribotoxin (XP_031030634.2) is an extracellular ribonuclease

that enter host cells and acts against the host ribosome. When compared to previous studies on the *F. oxysporum* secretome (Gámez-Arjona et al. 2022; Houterman et al. 2007), numerous additional potential virulence factors were identified: acyl transferase/acyl hydrolase/lysophospholipase (XP_031040750.1), peptidase S8/S53 domain-containing protein (XP_059466257.1), putative necrosis-inducing factor-domain-containing protein (XP_031038780.1), RlpA-like double-psi beta-barrel-protein domain-containing protein (XP_031046436.2), arabinan endo-1,5-alpha-L-arabinosidase A (XP_054562258.2), endoribonuclease L-PSP/chorismate mutase-like protein (XP_031045656.2, XP_031048984.2, XP_031049573.2), enolase (XP_031043713.1), NO signaling/golgi transport ligand-binding domain-containing protein (XP_059466819.1) and extradiol ring-cleavage dioxygenase, class III enzyme, subunit B (XP_031030589.2). Numerous potentially secreted hydrolases with a range of substrate specificities, so-called alpha/beta hydrolase proteins, were also found in our dataset (XP_031032669.2, XP_059468172.1, XP_031037010.2, XP_031037755.2, XP_031043170.2, XP_031044060.2, XP_031044516.2, XP_031046422.3, XP_031050083.2, XP_031051479.2, XP_054561888.2, XP_054562721.1, XP_054563059.1, XP_059465414.1, XP_059465699.1, XP_059465955.1, XP_059467372.1, XP_059467723.1, XP_059468182.1).

Discussion

Soil-borne pathogenic microorganisms are extremely difficult to combat. In order to reduce the incident of Fusarium crown and root-rot, an array of management strategies to reduce the inoculum density in the soil, to reduce the overall stress level in the plant and to adapt the soil environment are already well-described (Elmer 2015). One important part of an integrated pest management is the improvement of cultivar susceptibility to reduce the disease severity caused by Fusarium. However, highly resistant asparagus cultivars that could be used to improve plant health via breeding strategies are not available. Hence, this study aimed at a better understanding of infection-related systemic processes in asparagus in order to identify novel biomarkers that can be used for crop improvement. While the majority of scientific information on host–pathogen interaction originates from short-term infection studies on annual dicot model plants (Husaini et al. 2018), asparagus is a perennial monocot possessing intricate mechanisms triggered by pathogen attack. Further, the plant's response to pathogens is dependent on the infection stage, starting from early signaling events, induction of defense molecules and structures, up to programmed cell death (Husaini et al. 2018). Fusarium species are considered as hemibiotrophic pathogens because their infection cycle initiates as a biotroph and turns later into a necrotroph. In order to identify metabolite and protein markers for Fusarium-species defense responses in asparagus, the biotrophic stage of fungal growth was selected in this study, when the pathogens are actively colonizing the host and the host does not yet enter the final stage of infection.

Until now, metabolomic analyses in asparagus were focused mainly on profiling compounds with respect to quality traits (Creydt and Fischer 2020; Liu et al. 2022; Jiménez-Sánchez et al. 2016; Jaiswal et al. 2014; Dong et al. 2019) and food authentication (Creydt et al. 2018a, 2018b). With respect to plant pathogen interaction, so far, one study has reported on the metabolome and transcriptome alterations in asparagus with respect to stem blight disease caused by *Phomopsis asparagi* (Abdelrahman et al. 2020). Our study showed that, despite the production of Fusarium species-specific mycotoxins, the alterations in the asparagus metabolome were rather species-unspecific. We found an accumulation of compounds belonging to the pathway "Shikimates and Phenylpropanoids", acting as defense molecules, such as esculin, a phloem-mobile coumarin (Knox et al. 2018) with antioxidant and antimicrobial activities (Cai and Cai 2023). A further compound, chelidonic acid, was found only in the inoculated plants. Chelidonic acid was also found to accumulate in oil palm plants infected with the causal agent of basal stem rot, *Ganoderma boninense*, (Dzulkafli et al. 2019). Although the substance is of high pharmacological interest (Avdeeva et al. 2019), its exact role in plants remains to be elucidated. The enriched abundance of compounds involved in defense reactions was not reflected by an increased abundance of underlying biosynthetic proteins as revealed by the proteome data. Reasons for this effect could be transport processes within the plant from the place of synthesis

to the place of action, or the progressed stage of disease development where defense compounds are produced at a reduced rate. An increased abundance or de novo synthesis of several cytochrome P450 proteins was found upon infection, a diverse group of enzymes involved in developmental and stress-related processes, like phytohormone signaling, secondary metabolite and cell wall synthesis (Pandian et al. 2020; Xu et al. 2015). Since those proteins also play a role in detoxification of xenobiotics, it is reasonable to assume that those proteins enrich in response to the presence of mycotoxins or other fungal pathogenicity traits in stem bases.

Phytohormones play major roles in regulating defense responses and in principle, salicylic acid mediates resistance against biotrophic/hemibiotrophic pathogens, while jasmonic acid and ethylene signaling triggers resistance against necrotrophic pathogens. Abscisic acid seems to increase shoot disease symptoms (Di et al. 2016). This study showed that salicylic acid levels were not increased in stem bases, but rather its catabolite 2,3-dihydroxybenzoic acid and that high levels of the latter are connected to disease severity in roots. 2,3-dihydroxybenzoic acid is formed to prevent salicylic acid overaccumulation and is stored as sugar conjugates (Zhang et al. 2013). Recently it was found that also those glycosylated forms of 2,3-dihydroxybenzoic act as signaling molecules to initiate programed cell death in an hypersensitive response in *Arabidopsis* challenged with *Pseudomonas syringae* (Huang et al. 2018). One explanation for the missing higher abundance of salicylic acid in the inoculated plants could be that earlier reports are based on rather short-term inoculation experiments with incubations between some days and up to 8 weeks (He and Wolyn 2005, Waskiewicz et al. 2013, Hernández-Aparicio et al. 2021), while our experimental set-up lasted 12 weeks indicating that during disease progression, salicylic acid-based signaling might be replaced by other defense mechanisms. Further it is possible that levels of salicylic acid are reduced by the pathogen itself. It has been shown that *Fusarium graminearum* is able to degrade salicylic acid and uses it as carbon source (Rocheleau et al. 2019). However, transgenic strains of *F. graminearum* without the ability to catabolize salicylic acid produced the same disease symptoms on wheat spikelets as the wildtype strain, indicating that salicylic acid degradation is not required for pathogenicity (Rocheleau et al. 2019).

By far the largest group of compounds affected by the fungal infection was related to "Fatty acids", specifically the superclasses "Glycerophospholipids", "Glycerolipids" and "Sphingolipids", which were reduced in their abundance due to fungal infection. Concomitant, proteins involved in lipid metabolism and sphingolipid- and lipid-based signaling processes were lower abundant. Lipids play vital roles in fundamental metabolic processes such as membrane integrity, vesicle trafficking, endo- and exocytosis, signal transduction and plant immunity. During plant-pathogen interaction, host lipids act in jasmonic acid signaling pathway, programmed cell death, as structural barriers and as signaling molecules to further accelerate defense responses (Cavaco et al. 2021). Especially the role of sphingolipids in plant immunity is very well described for a number of pathosystems (Zeng and Yao 2022). *F. proliferatum*-produced FB1 is structurally similar to sphingoid bases sphinganine and sphingosine, with slightly different chain length, and is therefore able to inhibit plant ceramide synthase activity and disrupts sphingolipid metabolism. The results are induction of cell death, disruption of vacuolar membranes, endoplasmatic reticulum stress and impairment of plant growth (Zeng et al. 2020). A study on maize revealed that high accumulation of FB1 correlated with an increased abundance of sphinganine structures and glycerophospholipids, when compared to a low FB1 accumulating maize genotype (Righetti et al. 2021). We have found the reduction of glycerophospholipids, glycerolipids and sphingolipids in our study, irrespective of the presence of a specific mycotoxin, indicating that distortion of host lipid metabolism by Fusarium is a general infection process due to the action of additional virulence factors, such as secreted lipases.

Concomitant to our findings of reduced fatty acid-related compounds in response to Fusarium infection, proteome data revealed that proteins involved in vesicle formation and trafficking processes showed a reduced abundance upon fungal infection. Plant membrane trafficking pathways are prime targets of microbial pathogenic effector proteins with the aim to gain control of host cells by disrupting defense-related secretion and autophagy machinery, and by cytoskeletal reprogramming (Yuen et al. 2023). Vesicle-mediated cell detoxification of mycotoxins into plant vacuoles is an important resistance trait and impairment of this detoxification route significantly reduces mycotoxin tolerance and hence, resistance towards *F.*

graminearum and *Verticillium dahliae* (Wang et al. 2021). The strong impairment of vesicle-related processes in host plants by Fusarium, as observed in our data set, has not been reported so far, probably due to the performance of short-term infection experiments (Lyons et al. 2015; Zhang et al. 2023; Tu et al. 2023; Bhagat et al. 2024; Abdelrahman et al. 2020). This emphasizes the importance of long-term infection studies to fully understand plant-pathogen interactions. Potential biomarkers for improving asparagus resistance towards Fusarium could therefore include proteins involved in maintenance of vesicle fusion and autophagy machinery, as well as intracellular membrane trafficking for mycotoxin detoxification.

With respect to the proteome analyses, it became clear that the different Fusarium isolates had a high species-specific impact on the host proteome and that species-specificity was larger as seen in the metabolome data. This could be due to a Fusarium species-specific set of effector proteins. How the expression of particular fungal effector proteins affects the plant proteome was shown in a study on tomato. Here, *F. oxysporum* wildtype or knockout strains deficient in secreted effector proteins were used for plant infection. Proteome analysis of xylem sap showed that the absence of single effector proteins greatly affects plant responses (Gawehns et al. 2015). A previous study on different races of *F. oxysporum* using in planta RNA-sequencing revealed that each race expressed race-specific virulence factors although the disease phenotype was highly similar (Achari et al. 2021). Similar observations were made in our experiments where a large species-specific response on the plant proteome level was observed, while the disease phenotype in host plants was comparable. This could indicate that the plasticity of Fusarium virulence factors present in different Fusarium species enables the targeting of a large array of plant metabolic and cellular processes for a successful establishment within the host.

The proteome analysis identified fungal proteins within the plant samples. The higher number of proteins identified from *F. oxysporum* could be due to a higher genomic similarity between the isolate used in our experiments and the reference genome at NCBI, as compared with the isolates of *F. proliferatum* and *F. redolens*. The detected proteins reflect the repertoire of effector proteins that are described to affect plant infection: intracellular (SIX-proteins, ribonuclease/ribotoxin) and apoplastic proteins (Cerato-platanin-domain-containing protein, catalase-peroxidases) (Gutiérrez-Sánchez et al. 2023). However, 57% of the identified 1,488 fungal proteins lacked any functional annotation (see Supplemental Table 3). This underscores the need to study the Fusarium genus in more detail, especially with respect to the bioinformatical prediction of virulence factors to allow a more efficient disease control. In conclusion, we showed that Fusarium colonization of asparagus leads to disturbed lipid-based signaling processes, as well as dysfunctional vesicle formation, membrane integrity and cell wall organization in stem bases.

Acknowledgements We thank Mandy Heinze, Kerstin Fischer and Sieglinde Widiger for excellent technical assistance. We thank Susanne Bargen (Humboldt University of Berlin, Germany) and Christian Neubauer (University of Applied Sciences Osnabrück, Germany) and Reiner Krämer (Julius Kühn Institute Quedlinburg, Germany) for the gift of *Fusarium* spp. isolates.

Author contributions RDFK, RZ and KW designed the study and performed the plant inoculation experiments. VL, BC, HUH and SD performed the metabolome analyses and the respective data preparation. KW performed proteome analyses and respective data preparation. KW and RZ wrote the manuscript, with contributions from all authors. All authors read and approved the final manuscript.

Data availability All data supporting the findings of this study are available within the paper and its Supplementary Information.

Declarations

Conflict of interest The authors declare that the research was conducted in the absence of any commercial or financial relationships that could be construed as a potential conflict of interest.

Open Access This article is licensed under a Creative Commons Attribution 4.0 International License, which permits use, sharing, adaptation, distribution and reproduction in any medium or format, as long as you give appropriate credit to the original author(s) and the source, provide a link to the Creative Commons licence, and indicate if changes were made. The images or other third party material in this article are included in the article's Creative Commons licence, unless indicated otherwise in a credit line to the material. If material is not included in the article's Creative Commons licence and your intended use is not permitted by statutory regulation or exceeds the permitted use, you will need to obtain permission directly from the copyright holder. To view a copy of this licence, visit http://creativecommons.org/licenses/by/4.0/.

References

Abdelrahman M, Nakabayashi R, Mori T, Ikeuchi T, Mori M, Murakami K et al (2020) Comparative metabolome and transcriptome analyses of susceptible Asparagus officinalis and resistant wild A. kiusianus reveal insights into stem blight disease resistance. Plant Cell Physiol 61(8):1464–1476

Achari SR, Edwards J, Mann RC, Kaur JK, Sawbridge T, Summerell BA (2021) Comparative transcriptomic analysis of races 1, 2, 5 and 6 of *Fusarium oxysporum* f.sp. *pisi* in a susceptible pea host identifies differential pathogenicity profiles. BMC Genom 22(1). https://doi.org/10.1186/s12864-021-08033-y

Allwood JW, Williams A, Uthe H, van Dam NM, Mur LAJ, Grant MR et al (2021) Unravelling plant responses to stress - the importance of targeted and untargeted metabolomics. Metabolites 11(8):558

Andrzejak R, Janowska B (2021) The occurrence of *Fusarium* species in white spears of *Asparagus officinalis*. Notulae Botanicae Horti Agrobotanici Cluj-Napoca 49(4):12559

Andrzejak R, Janowska B (2022) The occurrence of Fusarium spp. in green Asparagus officinalis L. spears. Hortic Sci 4(4):234–247

Ashwin NMR, Barnabas L, Sundar AR, Malathi P, Viswanathan R, Masi A et al (2017) Advances in proteomic technologies and their scope of application in understanding plant-pathogen interactions. J Plant Biochem Biot 26(4):371–386

Avdeeva E, Shults E, Rybalova T, Reshetov Y, Porokhova E, Sukhodolo I et al (2019) Chelidonic acid and its derivatives from *Saussurea controversa*: Isolation, structural elucidation and influence on the osteogenic differentiation of multipotent mesenchymal stromal cells *in vitro*. Biomolecules 9:5

Baayen RP, van den Boogert P, Bonants PJM, Poll JTK, Blok WJ, Waalwijk C (2000) Fusarium redolens f.sp asparagi, causal agent of asparagus root rot, crown rot and spear rot. Eur J Plant Pathol 106(9):907–912

Bhagat N, Mansotra R, Patel K, Ambardar S, Vakhlu J (2024) Molecular warfare between pathogenic Fusarium oxysporum R1 and host Crocus sativus L. unraveled by dual transcriptomics. Plant Cell Rep 43:2

Borrego-Benjumea A, Basallote-Ureba MJ, Melero-Vara JM, Abbasi PA (2014) Characterization of Fusarium isolates from asparagus fields in Southwestern Ontario and influence of soil organic amendments on Fusarium Crown and Root Rot. Phytopathology 104(4):403–415

Cai T, Cai B (2023) Pharmacological activities of esculin and esculetin: a review. Medicine 102:40

Cavaco AR, Matos AR, Figueiredo A (2021) Speaking the language of lipids: the cross-talk between plants and pathogens in defence and disease. Cell Mol Life Sci 78(9):4399–4415

Creydt M, Fischer M (2020) Metabolic imaging: Analysis of different sections of white *Asparagus officinalis* shoots using high-resolution mass spectrometry. J Plant Physiol 250:153179

Creydt M, Arndt M, Hudzik D, Fischer M (2018a) Plant Metabolomics: evaluation of different extraction parameters for nontargeted UPLC-ESI-QTOF-mass spectrometry at the example of white *Asparagus officinalis*. J Agric Food Chem 66(48):12876–12887

Creydt M, Hudzik D, Rurik M, Kohlbacher O, Fischer M (2018b) Food authentication: small-molecule profiling as a tool for the geographic discrimination of German white asparagus. J Agric Food Chem 66(50):13328–13339

Di XT, Takken FLW, Tintor N (2016) How phytohormones shape interactions between plants and the soil-borne fungus *Fusarium oxysporum*. Front Plant Sci 7. https://doi.org/10.3389/fpls.2016.00170

DjalaliFarahani-Kofoet R, Witzel K, Gräfe J, Grosch R, Zrenner R (2020) Species-specific impact of *Fusarium* infection on the root and shoot characteristics of asparagus. Pathogens 9:6

Döll S, DjalaliFarahani-Kofoet R, Zrenner R, Henze A, Witzel K (2021) Tissue-specific signatures of metabolites and proteins in asparagus roots and exudates. Hortic Res 8:1

Dong TT, Han RP, Yu JW, Zhu MK, Zhang Y, Gong Y et al (2019) Anthocyanins accumulation and molecular analysis of correlated genes by metabolome and transcriptome in green and purple asparaguses (*Asparagus officinalis*, L.). Food Chem 271:18–28

Dührkop K, Fleischauer M, Ludwig M, Aksenov AA, Melnik AV, Meusel M et al (2019) SIRIUS 4: a rapid tool for turning tandem mass spectra into metabolite structure information. Nat Methods 16(4):299–302

Dührkop K, Nothias LF, Fleischauer M, Reher R, Ludwig M, Hoffmann MA et al (2021) Systematic classification of unknown metabolites using high-resolution fragmentation mass spectra. Nat Biotechnol 39(4):462–471

Dzulkafli SB, Othman A, Shahwan S, Nurazah Z, AbdManaf MA, Idris A et al (2019) Identification of chelidonic acid and asparagine in *Ganoderma boninense*-inoculated oil palm seedlings. J Oil Palm Res 31(1):53–66

Elmer WH (1990) *Fusarium proliferatum* as a causal agent in *Fusarium* crown and root-rot of asparagus. Plant Dis 74(11):938–938

Elmer WH (2015) Management of *Fusarium* crown and root rot of asparagus. Crop Protect 73:2–6

Feunang YD, Eisner R, Knox C, Chepelev L, Hastings J, Owen G et al (2016) ClassyFire: automated chemical classification with a comprehensive, computable taxonomy. J Cheminformatics 8. https://doi.org/10.1186/s13321-016-0174-y

Gámez-Arjona FM, Vitale S, Voxeur A, Dora S, Müller S, Sancho-Andrés G et al (2022) Impairment of the cellulose degradation machinery enhances *Fusarium oxysporum* virulence but limits its reproductive fitness. Sci Adv 8(16):eabl9734

Gawehns F, Ma LS, Bruning O, Houterman PM, Boeren S, Cornelissen BJC et al (2015) The effector repertoire of Fusarium oxysporum determines the tomato xylem proteome composition following infection. Front Plant Sci 6. https://doi.org/10.3389/fpls.2015.00967

Gutiérrez-Sánchez A, Plasencia J, Monribot-Villanueva JL, Rodríguez-Haas B, Ruíz-May E, Guerrero-Analco JA et al (2023) Virulence factors of the genus *Fusarium* with targets in plants. Microbiol Res 277:127506

He CY, Wolyn DJ (2005) Potential role for salicylic acid in induced resistance of asparagus roots to Fusarium oxysporum f.sp asparagi. Plant Pathol 54(2):227–232

He CY, Hsiang T, Wolyn DJ (2002) Induction of systemic disease resistance and pathogen defence responses in *Asparagus officinalis* inoculated with nonpathogenic strains of *Fusarium oxysporum*. Plant Pathol 51(2):225–230

Hernández-Aparicio F, Lisón P, Rodrigo I, Bellés JM, López-Gresa MP (2021) Signaling in the tomato immunity against *Fusarium oxysporum*. Molecules 26:7

Houterman PM, Speijer D, Dekker HL, de Koster CG, Cornelissen BJC, Rep M (2007) The mixed xylem sap proteome of *Fusarium oxysporum*-infected tomato plants. Mol Plant Pathol 8(2):215–221

Huang XX, Zhu GQ, Liu Q, Chen L, Li YJ, Hou BK (2018) Modulation of plant salicylic acid-associated immune responses via glycosylation of dihydroxybenzoic acids. Plant Physiol 176(4):3103–3119

Hulsen T, de Vlieg J, Alkema W (2008) BioVenn – a web application for the comparison and visualization of biological lists using area-proportional Venn diagrams. BMC Genomics 9(1):488

Husaini AM, Sakina A, Cambay SR (2018) Host-pathogen interaction in *Fusarium oxysporum* infections: where do we stand? Mol Plant-Microbe Interact 31(9):889–898

Iqbal M, Bibi Y, Iqbal Raja N, Ejaz M, Hussain M, Yasmeen F et al (2017) Review on therapeutic and pharmaceutically important medicinal plant *Asparagus officinalis* L. J Plant Biochem Phys 05:01

Jacobi J, Budahn H, Nothnagel T, Koenig J (2023) Studies on the identification of resistance to Fusarium oxysporum (Schlecht.) in different genetic backgrounds of Asparagus officinalis (L.) and its defense responses. Horticulturae 9(2):158

Jaiswal Y, Liang Z, Ho A, Chen H, Zhao Z (2014) A comparative tissue-specific metabolite analysis and determination of protodioscin content in asparagus species used in traditional Chinese medicine and Ayurveda by use of laser microdissection. UHPLC-QTOF/MS and LC-MS/MS Phytochem Anal 25(6):514–528

Jiménez-Sánchez C, Lozano-Sánchez J, Rodríguez-Pérez C, Segura-Carretero A, Fernández-Gutiérrez A (2016) Comprehensive, untargeted, and qualitative RP-HPLC-ESI-QTOF/MS2 metabolite profiling of green asparagus (*Asparagus officinalis*). J Food Comp Anal 46:78–87

Kanehisa M, Sato Y, Morishima K (2016) BlastKOALA and GhostKOALA: KEGG tools for functional characterization of genome and metagenome sequences. J Mol Biol 428(4):726–731

Keller-Pearson M, Bortolazzo A, Willems L, Smith B, Peterson A, Ané J-M et al (2023) A dual transcriptomic approach reveals contrasting patterns of differential gene expression during drought in arbuscular mycorrhizal fungus and carrot. Mol Plant-Microbe Interact 36(12):821–832

Kim HW, Wang MX, Leber CA, Nothias LF, Reher R, Kang KB et al (2021) NPClassifier: a deep neural network-based structural classification tool for natural products. J Nat Prod 84(11):2795–2807

Kind T, Wohlgemuth G, Lee DY, Lu Y, Palazoglu M, Shahbaz S et al (2009) FiehnLib: mass spectral and retention index libraries for metabolomics based on quadrupole and time-of-flight gas chromatography/mass spectrometry. Anal Chem 81(24):10038–10048

Kind T, Liu KH, Lee DY, DeFelice B, Meissen JK, Fiehn O (2013) LipidBlast *in silico* tandem mass spectrometry database for lipid identification. Nat. Methods 10(8):755

Knox K, Paterlini A, Thomson S, Oparkas K (2018) The coumarin glucoside, esculin, reveals rapid changes in phloem-transport velocity in response to environmental cues. Plant Physiol 178(2):795–807

Kolberg L, Raudvere U, Kuzmin I, Adler P, Vilo J, Peterson H (2023) g:Profiler-interoperable web service for functional enrichment analysis and gene identifier mapping (2023 update). Nucleic Acids Res 51(1):207–212

Ku YG, Bae JH, Namieśnik J, Barasch D, Nemirovski A, Katrich E et al (2018) Detection of bioactive compounds in organically and conventionally grown asparagus spears. Food Anal Meth 11(1):309–318

Lamondia JA, Elmer WH (1989) Pathogenicity and vegetative compatibility among isolates of *Fusarium oxysporum* and *Fusarium moniliforme* colonizing asparagus spears. Can J Bot-Rev Can Bot 67(8):2420–2424

Lanubile A, De Michele R, Loi M, Fakhari S, Marocco A, Paciolla C (2022) Cell death induced by mycotoxin fumonisin B_1 is accompanied by oxidative stress and transcriptional modulation in *Arabidopsis* cell culture. Plant Cell Rep 41(8):1733–1750

Lee JW, Lee JH, Yu IH, Gorinstein S, Bae JH, Ku YG (2014) Bioactive compounds, antioxidant and binding activities and spear yield of *Asparagus officinalis* L. Plant Foods Hum Nutr 69(2):175–181

Liu PX, Gao R, Gao L, Bi JX, Jiang YY, Zhang X et al (2022) Distinct quality changes of asparagus during growth by widely targeted metabolomics analysis. J Agric Food Chem 70(50):15999–16009

Lohse M, Nagel A, Herter T, May P, Schroda M, Zrenner R et al (2014) Mercator: a fast and simple web server for genome scale functional annotation of plant sequence data. Plant Cell Environ 37(5):1250–1258

Loi M, De Leonardis S, Mule G, Logrieco AF, Paciolla C (2020) A novel and potentially multifaceted dehydroascorbate reductase increasing the antioxidant systems is induced by beauvericin in tomato. Antioxidants 9:5

Lyons R, Stiller J, Powell J, Rusu A, Manners JM, Kazan K (2015) *Fusarium oxysporum* triggers tissue-specific transcriptional reprogramming in *Arabidopsis thaliana*. PLoS One 10:4

Mallebrera B, Prosperini A, Font G, Ruiz MJ (2018) *In vitro* mechanisms of Beauvericin toxicity: a review. Food Chem Toxicol 111:537–545

Mariscal M, Miguel-Rojas C, Hera C, Fernandes TR, Di Pietro A (2022) *Fusarium oxysporum* casein kinase 1, a negative regulator of the plasma membrane H^+-ATPase Pma1, is required for development and pathogenicity. J Fungi 8(12):1300

Mulè G, Susca A, Stea G, Moretti A (2004) A species-specific PCR assay based on the calmodulin partial gene for identification of Fusarium verticillioides, F. proliferatum and F. subglutinans. Eur J Plant Pathol 110(5–6):495–502

Mulè G, Susca A, Stea G, Moretti A (2004) Specific detection of the toxigenic species Fusarium proliferatum and F. oxysporum from asparagus plants using primers based

on calmodulin gene sequences. FEMS Microbiol Lett 230(2):235–240
Munkvold GP (2017) *Fusarium* species and their associated mycotoxins. Mycotoxigenic fungi: methods and protocols. 51–106. https://doi.org/10.1007/978-1-4939-6707-0_4
Pandian BA, Sathishraj R, Djanaguiraman M, Prasad PVV, Jugulam M (2020) Role of cytochrome P450 enzymes in plant stress response. Antioxidants 9:5
Pavlovkin J, Mistrikova I, Jaskova K, Tamas L (2012) Impact of beauvericin on membrane properties of young initial leaves of maize with different susceptibility to *Fusarium*. Plant Soil Environ 58(5):205–210
Righetti L, Dall'Asta C, Lucini L, Battilani P (2021) Lipid signaling modulates the response to fumonisin contamination and its source, *Fusarium verticillioides*, in maize. Front Plant Sci 12. https://doi.org/10.3389/fpls.2021.701680
Rocheleau H, Al-harthi R, Ouellet T (2019) Degradation of salicylic acid by *Fusarium graminearum*. Fungal Biol 123(1):77–86
Sawada Y, Nakabayashi R, Yamada Y, Suzuki M, Sato M, Sakata A et al (2012) RIKEN tandem mass spectral database (ReSpect) for phytochemicals: a plant-specific MS/MS-based data resource and database. Phytochemistry 82:38–45
Seefelder W, Gossmann M, Humpf HU (2002) Analysis of fumonisin B_1 in *Fusarium proliferatum*-infected asparagus spears and garlic bulbs from Germany by liquid chromatography-electrospray ionization mass spectrometry. J Agric Food Chem 50(10):2778–2781
Srobarova A, da Silva JAT, Kogan G, Ritieni A, Santini A (2009) Beauvericin decreases cell viability of wheat. Chem Biodivers 6(8):1208–1215
Sukumaran A, Woroszchuk E, Ross T, Geddes-McAlister J (2021) Proteomics of host-bacterial interactions: new insights from dual perspectives. Can J Microbiol 67(3):213–225
Sy-Cordero AA, Pearce CJ, Oberlies NH (2012) Revisiting the enniatins: a review of their isolation, biosynthesis, structure determination and biological activities. J Antibiot 65(11):541–549
Tu Q, Wang LR, An Q, Shuai J, Xia XB, Dong YF et al (2023) Comparative transcriptomics identifies the key *in planta*-expressed genes of *Fusarium graminearum* during infection of wheat varieties. Front Genet 14:1166832
Urbaniak M, Waśkiewicz A, Stępień Ł (2020) *Fusarium* cyclodepsipeptide mycotoxins: chemistry, biosynthesis, and occurrence. Toxins 12(12):765
Usadel B, Poree F, Nagel A, Lohse M, Czedik-Eysenberg A, Stitt M (2009) A guide to using MapMan to visualize and compare Omics data in plants: a case study in the crop species. Maize Plant Cell Environ 32(9):1211–1229
Wang D, Dong X (2011) A highway for war and peace: the secretory pathway in plant–microbe interactions. Mol Plant 4(4):581–587
Wang FL, Li XB, Li YJ, Han J, Chen Y, Zeng JY et al (2021) *Arabidopsis* P4 ATPase-mediated cell detoxification confers resistance to *Fusarium graminearum* and *Verticillium dahliae*. Nat Comm 12:1
Waskiewicz A, Irzykowska L, Drzewiecka K, Bocianowski J, Dobosz B, Weber Z et al (2013) Plant-pathogen interactions during infection process of asparagus with *Fusarium* spp. Cent Eur J Biol 8(11):1065–1076
Xu J, Wang XY, Guo WZ (2015) The cytochrome P450 superfamily: key players in plant development and defense. J Integr Agric 14(9):1673–1686
Yuen ELH, Shepherd S, Bozkurt TO (2023) Traffic control: subversion of plant membrane trafficking by pathogens. Annu Rev Phytopathol 61:325–350
Zeng HY, Li CY, Yao N (2020) Fumonisin B_1: a tool for exploring the multiple functions of sphingolipids in plants. Front Plant Sci 11. https://doi.org/10.3389/fpls.2020.600458
Zeng HY, Yao N (2022) Sphingolipids in plant immunity. Phytopathol Res 4:1
Zhang KW, Halitschke R, Yin CX, Liu CJ, Gan SS (2013) Salicylic acid 3-hydroxylase regulates *Arabidopsis* leaf longevity by mediating salicylic acid catabolism. Proc Natl Acad Sci U S A 110(36):14807–14812
Zhang H, Birch J, Pei J, Ma ZF, Bekhit AE-D (2019) Phytochemical compounds and biological activity in asparagus roots: a review. Int J Food Sci Tech 54(4):966–977
Zhang LL, Hou MW, Zhang XR, Cao YY, Sun SL, Zhu ZD et al (2023) Integrative transcriptome and proteome analysis reveals maize responses to *Fusarium verticillioides* infection inside the stalks. Mol Plant Pathol 24(7):693–710
Zrenner R, Genzel F, Verwaaijen B, Wibberg D, Grosch R (2020) Necrotrophic lifestyle of *Rhizoctonia solani* AG3-PT during interaction with its host plant potato as revealed by transcriptome analysis. Sci Rep 10:1
Zrenner R, Verwaaijen B, Genzel F, Flemer B, Grosch R (2021) Transcriptional changes in potato sprouts upon interaction with *Rhizoctonia solani* indicate pathogen-induced interference in the defence pathways of potato. Int J Mol Sci 22:6

Publisher's Note Springer Nature remains neutral with regard to jurisdictional claims in published maps and institutional affiliations.